Proportional Fair Resource Scheduling for Cell-Edge Users in O-RAN-Based Small-Cell Networks

Syed Tariq Shah*, Rana M. Sohaib†,Mahmoud A. Shawky ‡, Wali Ullah Khan§

*School of Computer Science & Electronic Engineering, University of Essex, Colchester, UK

Email: Syed.Shah@essex.ac.uk

† Department of Computer & Information Sciences, Northumbria University, UK

Email: Rana.Sohaib@northumbria.ac.uk,

‡James Watt School of Engineering, University of Glasgow, Glasgow, UK

Email: Mahmoud.Shawky}@glasgow.ac.uk

§ Interdisciplinary Centre for Security, Reliability and Trust (SnT), University of Luxembourg, Luxembourg

Email: Waliullah.Khan@uni.lu

***Abstract*—This paper introduces a novel strategy for radio resource scheduling in a Coordinated Multi-Point (CoMP) Open Radio Access Network (O-RAN) environment, particularly under the constraints of a non-ideal fronthaul. We propose a comprehensive three-phase scheme, which includes the selection of Cell Edge Users (CEUEs), DPS-based clustering and switching, and a weighted mechanism for Proportional Fair (PF)-based radio resource allocation. Using a modified Vienna 5G system-level simulator, we conducted a series of detailed simulations to validate our approach in a real-world scenario. The simulation results reveal significant enhancements in both the throughput performance of CEUEs and the overall user average throughput. Furthermore, our approach demonstrates substantial improvements in the fairness index, thereby underscoring its potential to significantly improve the efficiency and user experience within 5G networks.**

***Index Terms*—Open-RAN, Cell-edge UEs, 5G, Small Cell, Resource Allocation**

I. INTRODUCTION

The advent of new and advanced use cases, such as extended reality, multisense interfaces, holograms, and high-speed video services, is driving a rapid evolution in mobile network technologies. Anticipated to be mainstream in the next decade, these applications demand networks capable of supporting 1-10 Gbit/s bandwidth per user, latencies as low as 1-5 ms, and near-perfect availability of 99.999% [1], [2]. However, current network architectures fall short of these requirements, necessitating the adoption of new paradigms such as densely populated small cell networks and the Open Radio Access Network (O-RAN). The O-RAN with small cells technology, recognised for its layered and modular design, offers a flexible and cost-effective solution to cater to these emerging needs [3].

A critical challenge in these densely populated network environments is the phenomenon of cell-edge user equipment (CEUEs), which often experience degraded service quality due to factors like inter-cell interference and signal attenuation. To address this, Coordinated Multi-Point (CoMP) transmission and reception has emerged as a key technology [4]. CoMP enhances the performance of CEUEs by efficiently coordinating multiple neighbouring Transmission Reception Points (TRPs), thereby improving CEUEs throughputs [5]–[7]. Despite its advantages, the performance of CoMP is significantly constrained by the limitations of fronthaul or backhaul bandwidth [8], [9]. This bottleneck is further exacerbated by the redundant data transmissions inherent in CoMP, which place additional load on the fronthaul network, compromising the overall efficiency of Centralized Radio Access Networks (C-RANs) [10], [11].

The implementation of CoMP in O-RAN, especially under non-ideal fronthaul conditions, introduces additional complexities in resource scheduling [9], [12]. The fluctuating fronthaul bandwidth, influenced by the wireless side's resource allocation strategy, critically impacts the transmission efficiency [13], [14]. Prior research in this area has explored various approaches to radio resource allocation in CoMP C-RAN [4], including novel packet delivery mechanisms and time-frequency resource allocation tailored for Ultra-Reliable Low-Latency Communications (URLLC) [15]. However, these studies have predominantly considered scenarios with fixed fronthaul links, thus not addressing the nuanced challenges presented by CoMP in O-RAN with non-ideal fronthaul. In this context, Dynamic Point Selection (DPS) becomes pivotal in 5G networks, serving as a mechanism to enhance transmission quality and Quality of Service (QoS) by efficiently coordinating multiple transmission points [16], [17]. Studies have shown that DPS, when implemented in CoMP, can significantly improve cell-edge throughputs, outperforming traditional LTE approaches [7]. A generic DPS scenario, with 2 TRPs forming a cluster in O-RAN, is depicted in Fig. 1.

This paper aims to address these gaps by introducing a novel resource scheduling strategy tailored for CoMP in O-RAN-based small-cell networks, particularly under non-ideal fronthaul conditions. We propose an approach that not only accommodates the high-density and dynamic nature of modern networks but also ensures efficient resource management and efficient service delivery to cell-edge users. Our contribution lies in the introduction of a three-phase resource allocation scheme that encompasses the selection of CEUEs, DPS-based clustering and switching, and an innovative Proportional Fair (PF)-based radio resource allocation mechanism. This scheme is meticulously designed to address the unique challenges of non-ideal fronthaul and the complexities of Split 6 architecture in O-RAN systems. To validate the effectiveness of our proposed model, we employ a modified Vienna 5G System Level Simulator for a comprehensive system-level simulation in a real-world scenario.The extensive simulation results indicate that our approach significantly improves the CEUE and throughput performance and resource allocation fairness index compared to conventional strategies, resulting in a substantial leap forward in enhancing 5G network efficiency and user experience.

The remainder of this paper is organized as follows: Section II provides a comprehensive overview of the system model, which includes the architecture of the multi-cell 5G network based on O-RAN, along with specific considerations for coordinated multipoint (CoMP) and non-ideal fronthaul. In Section III, we introduce our proposed scheme and elaborate on the resource allocation algorithm we developed. Section IV details the methodology and setup of our extensive simulations, presenting the results obtained. Finally, Section V concludes the paper by summarizing the key findings.

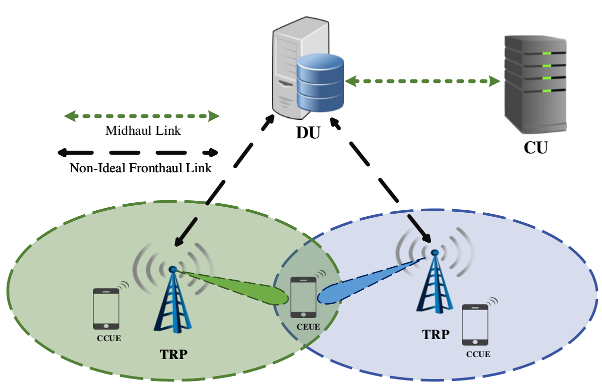

Fig. 1: Generic DPS scenario, with 2 TRPs forming a cluster in O-RAN.

II. System Model

We consider the downlink of a multi-cell 5G network based on O-RAN where four single-sector open-radio units (O-RUs) are deployed on the vertices of a square such that the minimum inter-RU distance, D, is 150m. The Distributed Unit (DU) is assumed to be in the centre of the square area and connects to each RU via a non-ideal mmWave fronthaul link operating in 57 – 71 GHz. Each sector in the network is considered to be a transmission-reception-point (TRP) with N transmit antennas. Note that the terms TRP and O-RU are used interchangeably in this manuscript. Accordingly, each TRP is mapped to a unique SSB index such that TRPIdx = SSBIdx. The timing intervals of the SSB bursts are determined by the chosen subcarrier spacing numerology. We employ numerology 1 (SCS 30 KHz), with a carrier frequency of 3.5 GHz, transmitting 8 SSBs within a 5 ms window. A designated beam is emitted in a particular direction to transmit each SSB. Each UE can detect each SSB beam and identify the SSB index with the strongest RSRP value. UE evaluates the RSRP of every detected SSB during a specific time frame. It is further assumed that there is one PRACH slot in every subframe with msg1-FDM = 1 and ssb-perRACH-OccasionAndCB-PreamblesPerSSB = $\{8, 8\}$ or $\{4, 16\}$, which allows for a unique one-to-one mapping of each SSB to a RACH Occasion and supported by PrachCfgIdx =157 or 162 configuration. K multi-antenna users are assumed to be uniformly distributed within the coverage area.

A. Slot Format and HARQ process

A TDD system with a slot format of 7D-1S-2U, where S = 12D-2G is assumed, as shown in Figure 2. With a maximum HARQ Round Trip Time (RTT) of 8ms $(16 \times 0.5$ ms), feedback for all HARQ processes within the half-frame is transmitted by UEs in the last subframe [18]. The downlink slots are configured with decreasing K1 values starting from K1 = 9 in the first TS in a half-frame to K1=3 in the 7th TS (last DL slot) of the half-frame. K1 refers to the time delay between the downlink slot and the uplink slot. For a HARQ process in TS 1, this corresponds to 4.5ms between data leaving the DU and when the UE transmits its HARQ feedback. With nFAPI frame advance, frame build and UE processing adding up to 1ms, this leaves 3.5ms for a non-ideal fronthaul link, which is more than the 2ms target and has a higher probability of success. Given that the maximum HARQ RTT is 8ms, HARQ feedback from the UE has 3.5ms to get back to the DU, which is also more than the fronthaul latency target. For the 7th TS in the half-frame with K1 = 3, the fronthaul latency budget is 0.5ms, which is less than the target and has a low probability of success. The success probability for each HARQ transmission can be modelled based on the BER [18], [19]. A transmission is deemed successful when the received bits are decoded correctly. To estimate the probability of success for each attempt, we can use the cumulative distribution function (CDF) of the bit error rate (BER). With the probabilities of each K1 value established, we conduct a Bernoulli experiment to determine whether the Transport Block (TB) sent to each user in every transmission slot (TS) is successful. Transmissions are considered unsuccessful if the feedback cannot be received by the network within the K1 duration; in such cases, the network must retransmit the TB in the following TS.

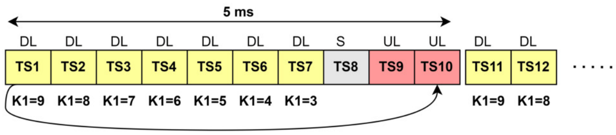

Fig. 2: TDD slot format and K1 values

III. Proposed Scheme

The proposed scheme consists of three main phases, i.e., DPS-based clustering and switching, CEUE selection, and PF-based radio resource allocation. The details of each phase are thoroughly discussed in the subsections given below.

A. DPS-based clustering and switching

The proposed scheme then executes the DPS phase to perform an efficient DPS operation. In order to do so it is necessary to determine which neighbouring TRPs can be part of the cluster that can best support candidate CEUEs. With this intention, the DU defines the DPS cluster for each CEUE based on the CQI from its neighbouring TRPs. Depending on the cluster's size, the DU selects the TRPs with the best CQI to form a cluster for all CEUEs in the network. Based on (2), the CQI for each UE from a particular TRP can be calculated according to [20].

Moreover, in our proposed scheme, the clustering is performed after every l frame. Likewise, since the users in our proposed system model are considered to be moving, the TRP switching (i.e., switching to a new TRP in the cluster) is performed after every m number of frames. During a switching slot, the CEUE only switches to a new TRP in the cluster when the CQI from the other TRPs in the cluster is better than the CQI of the associated TRP. Note that in our proposed scheme, the cluster size, clustering periodicity (i.e., after how many frames the clustering is performed), and switching periodicity (i.e., after how many frames the switching is performed) are kept variable. The network operators can set these variables depending on the deployed network's density and specific system model.

B. Cell Edge UE Selection

In our proposed RRM scheme, once clustering is done, the DU classifies UEs into CCUEs and CEUEs based on their received SINR. More specifically, the DU calculates the received SINR of each UE and compares it with a predefined threshold SINR; if the received SINR is lower than the threshold, the UE is classified as CEUE; otherwise, it is classified as CCUE. Mathematically, it can be expressed as

$$C(\gamma_i^{UE}) = \begin{cases} \text{CEUE} & \text{if } \gamma_i^{UE} < \gamma_{th} \\ \text{CCUE} & \text{if } \gamma_i^{UE} \geq \gamma_{th} \end{cases}, \quad (1)$$

where γ_i^{UE} is the received SINR of i^{th} UE in the network and can be calculated as

$$\gamma_i^{UE} = \frac{p_{g,i}^n, h_{g,i}^n}{I_{g,i}^n + N_o B}. \quad (2)$$

In (2), $p_{g,i}^n$ and $h_{g,i}^n$ refers to the transmit power and channel coefficient of i^{th} UE on resource block n associated to O-RU g served by an O-DU/TRP, respectively. Whereas N_o indicate the power spectral density of Gaussian noise, and B is the bandwidth. $I_{g,i}^n$ refers to the co-channel interference. Note that for the rest of the paper, the set of CEUEs and CCUEs is represented by $\boldsymbol{CEUEs} = \{CEUE_1, \cdots CEUE_X\}$, and $\boldsymbol{CCUEs} = \{CCUE_1, \cdots CCUE_Y\}$, respectively. Where X and Y are the total numbers of CEUEs and CCUEs, respectively. Likewise the total number of UEs can be represented by N such that $N = X + Y$.

Data: **UEs**
if *clustering frame* **then**
  Execute Clustering Procedure
else
  Execute Switching Procedure
end
for $i = 1$ **to** N **do**
  Calculate $SINR_{UE_i}$ for each UE_i
end
Initialize: $\mathbf{CEUEs} = \emptyset$, $\mathbf{CCUEs} = \emptyset$
for $i = 1$ **to** N **do**
  if $SINR_{UE_i} < \gamma_{thr}$ **then**
    Append UE_i to $\mathbf{CEUEs}$ (Cell-Edge UEs)
  else
    Append UE_i to $\mathbf{CCUEs}$ (Cell-Center UEs)
  end
end
Note: $\mathbf{UEs} = \{\mathbf{CEUEs}, \mathbf{CCUEs}\}$,
$\mathbf{CEUEs} = \{CEUE_1, \ldots, CEUE_X\}$,
$\mathbf{CCUEs} = \{CCUE_1, \ldots, CCUE_Y\}$, $N = X + Y$
for $i = 1$ **to** N **do**
  Calculate $\delta_{UE,i}$ for each UE_i
end
Construct candidate UEs list $\mathbf{CUEs}$ by sorting $\mathbf{UEs}$ in descending order of δ_{UEs} values
for *time slot* $j = 1$ **to** J **do**
  Select the first n UEs from $\mathbf{CUEs}$ for resource allocation
  Set: $\mathbf{SUEs} = \{SUE_1, \ldots, SUE_n\} = \{\bar{\mathbf{X}} = \{CEUE_1, \ldots, CEUE_x\}, \bar{\mathbf{Y}} = \{CCUE_1, \ldots, CCUE_y\}\}$
  Note: $\bar{\mathbf{X}} \subseteq \mathbf{CEUEs}$, $\bar{\mathbf{Y}} \subseteq \mathbf{CCUEs}$, $\bar{N} = |\bar{\mathbf{X}}| + |\bar{\mathbf{Y}}|$
  Calculate weight factors ω_{SUE_i} for all UEs in $\mathbf{SUEs}$
  for $i = 1$ **to** $\bar{N}$ **do**
    if $SUE_i \in \bar{\mathbf{X}}$ **then**
      $\omega_{SUE_i} = \frac{\rho}{N} + \frac{(1-\rho) \times \delta_{SUE_i}}{\sum_{k=1}^{|\bar{\mathbf{X}}|} \delta_{SUE_k}}$
      Append ω_{SUE_i} to $\omega_{\mathbf{SUE}}$
    else
      $\omega_{SUE_i} = \frac{\rho}{N}$
      Append ω_{SUE_i} to $\omega_{\mathbf{SUE}}$
    end
  end
  for $SUE_i \in \mathbf{SUEs}$ **do**
    Allocate radio resources to all users in $\mathbf{SUEs}$ proportional to ω_{SUE}:
    $\lambda_{SUE_i} = \omega_{SUE_i} \cdot \Lambda_T$
  end
end

Algorithm 1: Proposed Radio Resource Allocation Algorithm

C. PF-based Candidate UE Selection and Radio Resource Allocation

We consider that many UEs are present in the network, but only a specific number of deserving UEs can be selected for resource allocation during each slot. The selection of a number of UEs per TS in the proposed scheme depends on various factors. Factors such as interference, resource allocation efficiency, and the available bandwidth can influence the decision to limit the number of scheduled UEs per TS. Managing interference becomes more challenging as the number of scheduled UEs increases. Limiting the number of UEs per TS can help mitigate interference issues and can also help meet stringent latency requirements for URLLC services [2], [12]. In our proposed approach, we configured it to allocate resources for up to 8 UEs in a given TS.

At the commencement of each frame, the proposed algorithm dynamically decides between clustering and switching procedures, contingent on the frame type. This bifurcation is crucial for enhancing resource allocation based on the network's current state. Subsequently, the algorithm embarks on the computation of the SINR for all connected UEs. This step is pivotal in assessing the channel quality experienced by each UE. As mentioned earlier, following the SINR calculation, the algorithm segregates the UEs into two distinct sets: **CEUEs** and **CCUEs**. This classification is based on the SINR values, with a predefined threshold (γ_{thr}) serving as the demarcation criterion. These operations are encapsulated in steps 1 through 3 of Algorithm 1.

The next phase involves the computation of the PF metric for each UE [21], [22]. The PF metric, a critical component of our proposed scheme, can be calculated as follows

$$\delta_{UE,i} = 1 + \frac{r_{UE_i}}{R_{UE_i}}, \tag{3}$$

where r_{UE_i} is the achievable throughput of i^{th} UE and R_{UE_i} is its historical throughput. The PF metric plays a fundamental role in ensuring a fair and efficient allocation of resources by considering both the current channel conditions and the historical throughput of each UE. Upon calculating PF metrics, the UEs are methodically arranged in descending order based on their PF values, forming the candidate UEs set (**CUEs**).

$$\delta_{UE,i} = 1 + \frac{r_{UE_i}}{R_{UE_i}}, \tag{4}$$

Before the actual allocation of radio resources, the algorithm computes a weight metric for each UE in the selection pool. In every time slot, the algorithm selects the top $\bar{N}$ UEs from the **CUEs** list for resource allocation. The selected UEs can be defined in a set $\mathbf{SUEs} \ni \mathbf{SUEs} = \{SUE_1, \ldots, SUE_n\} = \{\bar{\mathbf{X}} = \{CEUE_1, \ldots, CEUE_x\}, \bar{\mathbf{Y}} = \{CCUE_1, \ldots, CCUE_y\}\}$ where $\bar{\mathbf{X}} \subseteq \mathbf{CEUEs}$, $\bar{\mathbf{Y}} \subseteq \mathbf{CCUEs}$, and $\bar{N} = |\bar{\mathbf{X}}| + |\bar{\mathbf{Y}}|$.

Once the selected UEs are segregated in CEUEs $\bar{\mathbf{X}}$ and CCUEs $\bar{\mathbf{Y}}$, the algorithm then calculates a weight factor (ω_{SUE_i}), for all $\bar{N}$ UEs. More specifically, the (ω_{SUE_i}) for CEUEs $\bar{\mathbf{X}}$ is calculated in following manner

$$\omega_{SUE_i} = \frac{\rho}{\bar{N}} + \frac{(1-\rho) \times \delta_{SUE_i}}{\sum_{k=1}^{|\bar{\mathbf{X}}|} \delta_{SUE_k}}. \tag{5}$$

Likewise, for CCUEs in set $\bar{\mathbf{X}}$ the ω_{SUE_i} is calculated in the following manner

$$\omega_{SUE_i} = \frac{\rho}{\bar{N}}. \tag{6}$$

Note that in both (5) and (6), the ρ is the weight factor. In other words, ρ can be used to prioritise CECUEs or CCUEs while deciding the number of allocated radio resources. Moreover, from (5), it can also be observed that among selected CEUEs ($\bar{\mathbf{X}}$), the proposed scheme further prioritises the CEUEs with higher PF metric values. This weighted factor is adopted to ensure that the deprived CEUEs among selected CEUES receive more radio resources than other selected UEs.

TABLE I: Simulation Parameters

Parameter	**Value**
Carrier frequency	3.5 GHz
Subcarrier spacing	30 KhZ
BS antenna height	5 m
Bandwidth	40 MHz
BS receiver noise figure	4 dB
No. of TRPs/cluster	2
SSB periodicity	10 ms
Antenna gain	17 dBi
No. of UEs/TS	8
UE receiver noise figure	9 dB
UE speed	3 km/h
UE attachment	SINR-based
Traffic model	Full buffer
Equaliser	MMSE
l	1 Frame
TRP transmission power	34 dBm
Path Loss	3GPP 38.901 UMi LOS
Channel	PedA model
Max HARQ RTT	8 ms
m	2 Frames

IV. Simulation Results

We consider a specific scenario of University Avenue, Glasgow where four TRPs are strategically positioned to ensure comprehensive coverage, as shown in Fig 3. The depiction is based on a realistic map of University Avenue, Glasgow, incorporating RUs to simulate and test the performance of the Open-RAN network in the region. The performance of the proposed algorithm is evaluated using a modified Vienna 5G System Level Simulator [23]. The simulation parameters are provided in Table I.

In the final step, after the weights are calculated, the proposed algorithm then allocates the radio resource to all selected UEs (**SUEs**) based on their weights in the following manner

$$\lambda_{SUE_i} = \omega_{SUE_i} \cdot \Lambda_T, \tag{7}$$

where λ_{SUE_i} is the resources allocated to i^{th} SUE and Λ_T is the total number of available resources in the network.

The bar chart in Fig. 4 illustrates the comparative average throughput performance of cell edge users under three distinct resource schedulers. The first bar denotes the average throughput performance utilising our proposed PF-based scheduling algorithm, achieving the highest throughput of

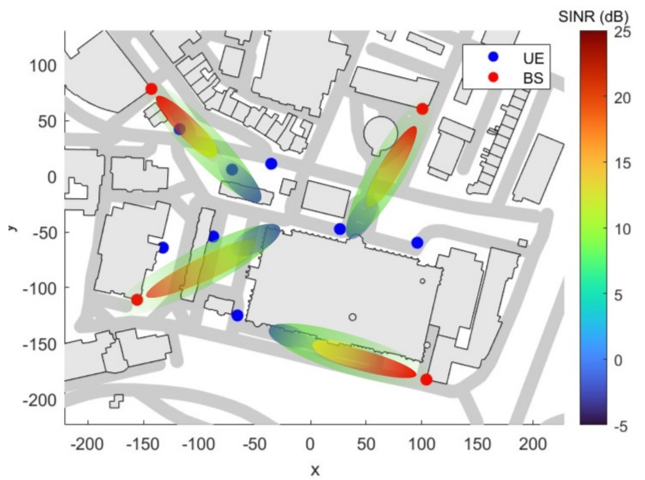

Fig. 3: Illustration of the University Avenue, Glasgow scenario, with 4 TRPs placed in the area ensuring thorough coverage.

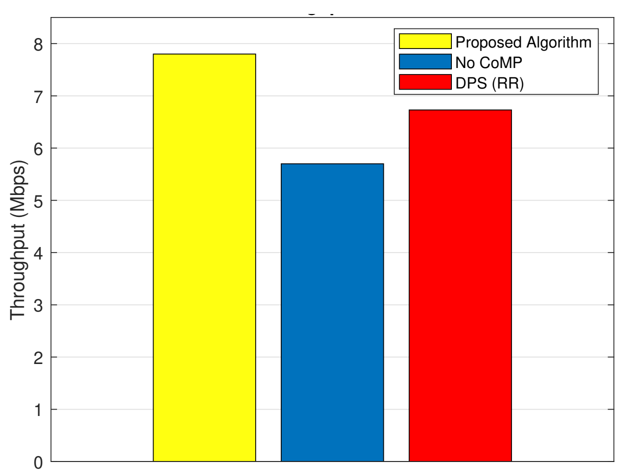

Fig. 4: CEUE Average Throughput Performance

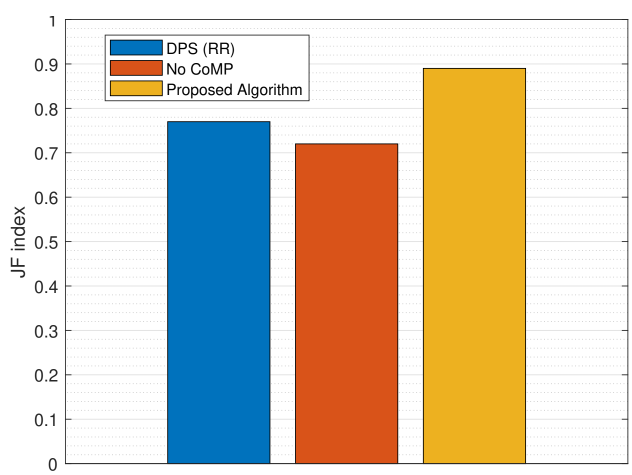

Fig. 5: Jain's Fairness Index

just over 7.8 Mbps. In contrast, the second bar represents a baseline where no CoMP strategies are implemented, resulting in a reduced average throughput of approximately 5.6 Mbps. More specifically, no CoMP refers to the scheduling scheme where CEUEs are not classified or prioritised, and radio resources among all UEs are distributed in a round-robin (RR) manner. The third bar shows the CEUE's average throughput where clustering and switching features of DPS CoMP are implemented, but radio resources are distributed among all selected UEs in an RR fashion. Based on the results in Fig. 4, it can be observed that in terms of CEUE throughput, the proposed scheme outperforms the baseline schemes. This is because the proposed scheme utilizes a PF-based scheduler and prioritizes the deprived CEUEs by adopting a weighted mechanism. This assigns higher weights to CEUEs with higher PF metric values, resulting in higher average throughput for CEUEs in the proposed scheme than in the baseline schemes.

Likewise, the results depicted in Fig. 5 provide an insightful comparison of Jain's Fairness Index between the proposed scheme and baseline schemes. To evaluate the distribution of throughput across UEs, Jain's fairness index was employed as defined in [24]. The Jain's fairness index ($\mathbf{J}$) is given by

$$\mathbf{J}(\omega_1, \omega_2, \ldots, \omega_N) = \frac{(\sum_{i=1}^{N} \omega_i)^2}{N \sum_{i=1}^{N} \omega_i^2}, \quad (8)$$

where ω_i represents the throughput of the i-th UE, and N is the total number of UEs. The index value lies between 0 and 1, where values closer to 1 indicate a higher level of fairness in radio resource distribution. The proposed scheme achieves significantly better performance than the other two baseline schemes in terms of fairness. This performance superiority is primarily attributed to its use of a PF-based scheduler, coupled with a strategic focus on disadvantaged CEUEs. Since the scheme adopts a weighted mechanism, greater weights are allocated to CEUEs that exhibit higher PF metric values. Consequently, this approach leads to a notable enhancement in the fairness index when compared to the baseline alternatives, where resources are equally distributed among all users in a round-robin manner and CEUEs are identified or prioritised.

The Cumulative Distribution Function (CDF) plot in Fig. 6 compares the distribution of the average throughput across all UEs in the network following a clustering period. The CDF illustrates the proportion of UEs that achieve a certain throughput threshold, providing a comprehensive view of network performance.

The results indicate that a greater percentage of UEs achieve higher average throughputs under the proposed algorithm than no-CoMP and DPS-RR strategies. It implies that the proposed algorithm is effective not only in raising the overall throughput but also in ensuring that a more significant portion of UEs experiences high data rates. To this end, the CDF plot clearly demonstrates that the Proposed Algorithm outperforms the baseline no-CoMP and DPS-RR scenarios in terms of delivering higher average throughput

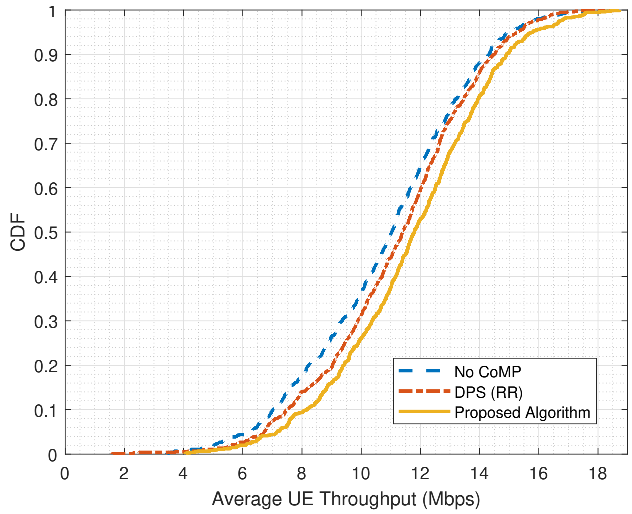

Fig. 6: Average UE throughput after two frames clustering

to UEs in the network. In other words, this suggests that the Proposed Algorithm could offer a more equitable distribution of network resources and a better quality of service for all connected UEs.

V. Conclusion

In conclusion, this paper presents a comprehensive and innovative approach to addressing the challenges of resource scheduling in O-RAN architectures with CoMP and non-ideal fronthaul conditions. Our proposed scheme, encompassing CEUE selection, DPS-based clustering and switching, and PF-based radio resource allocation, demonstrates a significant enhancement in network performance. The simulation results, based on a realistic scenario at University Avenue, Glasgow, underscore the practical applicability and effectiveness of our approach. The proposed algorithm not only improves the average throughput for cell-edge users but also ensures a more equitable distribution of network resources, as evidenced by the improved Jain's fairness index.

References

[1] R. Li *et al.*, "Towards a new internet for the year 2030 and beyond," in *Proc. 3rd Annu. ITU IMT-2020/5G Workshop Demo Day*, 2018, pp. 1–21.

[2] R. M. Sohaib, S. Tariq Shah, and P. Yadav, "Towards resilient 6g o-ran: An energy-efficient urllc resource allocation framework," *IEEE Open Journal of the Communications Society*, vol. 5, pp. 7701–7714, 2024.

[3] H. Zhang, H. Zhou, and M. Erol-Kantarci, "Team learning-based resource allocation for open radio access network (o-ran)," in *ICC 2022 - IEEE International Conference on Communications*, 2022, pp. 4938–4943.

[4] S. T. Shah, J. S. Kim, E. S. Bae, J. Bae, and M. Y. Chung, "Radio resource management for 5g mobile communication systems with massive antenna structure," *Transactions on Emerging Telecommunications Technologies*, vol. 27, no. 4, pp. 504–518, 2016.

[5] P. Yang, L. Chen, H. Zhang, J. Yang, R. Wang, and Z. Li, "Joint optical and wireless resource allocation for cooperative transmission in c-ran," *Sensors*, vol. 21, no. 1, 2021. [Online]. Available: https://www.mdpi.com/1424-8220/21/1/217

[6] M. S. J. Solaija, H. Salman, A. B. Kihero, M. I. Sağlam, and H. Arslan, "Generalized coordinated multipoint framework for 5g and beyond," *IEEE Access*, vol. 9, pp. 72 499–72 515, 2021.

[7] H.-L. Määttänen, K. Hämäläinen, J. Venäläinen, K. Schober, M. Enescu, and M. Valkama, "System-level performance of lte-advanced with joint transmission and dynamic point selection schemes," *EURASIP Journal on Advances in Signal Processing*, vol. 2012, pp. 1–18, 2012.

[8] Q. Wang, Y. Liu, Y. Wang, X. Xiong, J. Zong, J. Wang, and P. Chen, "Resource allocation based on radio intelligence controller for open ran toward 6g," *IEEE Access*, vol. 11, pp. 97 909–97 919, 2023.

[9] M. Karbalaee Motalleb, V. Shah-Mansouri, S. Parsaeefard, and O. L. Alcaraz López, "Resource allocation in an open ran system using network slicing," *IEEE Transactions on Network and Service Management*, vol. 20, no. 1, pp. 471–485, 2023.

[10] L. You and D. Yuan, "Joint comp-cell selection and resource allocation in fronthaul-constrained c-ran," in *2017 15th International Symposium on Modeling and Optimization in Mobile, Ad Hoc, and Wireless Networks (WiOpt)*. IEEE, 2017, pp. 1–6.

[11] M. Moltafet, N. Mokari, R. Joda, M. R. Sabagh, and M. Zorzi, "Joint access and fronthaul resource allocation in dual connectivity and comp based networks," in *2018 IEEE International Conference on Communications (ICC)*, 2018, pp. 1–6.

[12] R. M. Sohaib, S. T. Shah, O. Onireti, Y. Sambo, Q. H. Abbasi, and M. A. Imran, "Drl-based joint resource scheduling of embb and urllc in o-ran," in *2024 IEEE International Conference on Communications Workshops (ICC Workshops)*, 2024, pp. 1523–1528.

[13] Y. Qi, M. Z. Shakir, M. A. Imran, K. A. Qaraqe, A. Quddus, and R. Tafazolli, "Fronthaul data compression for uplink comp in cloud radio access network (c-ran)," *Transactions on Emerging Telecommunications Technologies*, vol. 27, no. 10, pp. 1409–1425, 2016.

[14] Y. Tian, K.-L. Lee, C. Lim, and A. Nirmalathas, "Performance evaluation of comp for downlink 60-ghz radio-over-fiber fronthaul," in *2017 International Topical Meeting on Microwave Photonics (MWP)*, 2017, pp. 1–4.

[15] J. Khan and L. Jacob, "Resource allocation for comp enabled urllc in 5g c-ran architecture," *IEEE Systems Journal*, vol. 15, no. 4, pp. 4864–4875, 2021.

[16] V. I. Tatsis, M. Karavolos, D. N. Skoutas, N. Nomikos, D. Vouyioukas, and C. Skianis, "Energy-aware clustering of comp-dps transmission points," *Computer Communications*, vol. 135, pp. 28–39, 2019.

[17] S. Mondal and M. Ruffini, "Fairness guaranteed and auction-based x-haul and cloud resource allocation in multi-tenant o-rans," *IEEE Transactions on Communications*, vol. 71, no. 6, pp. 3452–3468, 2023.

[18] N. Strodthoff, B. Göktepe, T. Schierl, C. Hellge, and W. Samek, "Enhanced machine learning techniques for early harq feedback prediction in 5g," *IEEE Journal on Selected Areas in Communications*, vol. 37, no. 11, pp. 2573–2587, 2019.

[19] N. Strodthoff, B. Göktepe, T. Schierl, W. Samek, and C. Hellge, "Machine learning for early harq feedback prediction in 5g," in *2018 IEEE Globecom Workshops (GC Wkshps)*, 2018, pp. 1–6.

[20] 3rd Generation Partnership Project (3GPP), "Evolved universal terrestrial radio access (e-utra); physical layer procedures," 3GPP, Tech. Rep. TS 36.213., Jan 2015.

[21] S. T. Shah, J. Gu, S. F. Hasan, and M. Y. Chung, "Proportional fair scheduling using water-filling technique for sc-fdma based d2d communication," *Physical Communication*, vol. 59, p. 102108, 2023.

[22] S. T. Shah, S. F. Hasan, J. Gu, and M. Y. Chung, "Sc-fdma-based resource allocation and power control scheme for d2d communication using lte-a uplink resource," *EURASIP Journal on Wireless Communications and Networking*, vol. 2015, no. 1, pp. 1–15, 2015.

[23] M. K. Müller, F. Ademaj, T. Dittrich, A. Fastenbauer, B. R. Elbal, A. Nabavi, L. Nagel, S. Schwarz, and M. Rupp, "Flexible multi-node simulation of cellular mobile communications: the Vienna 5G System Level Simulator," *EURASIP Journal on Wireless Communications and Networking*, vol. 2018, no. 1, p. 17, Sep. 2018.

[24] R. K. Jain, D.-M. W. Chiu, W. R. Hawe *et al.*, "A quantitative measure of fairness and discrimination," *Eastern Research Laboratory, Digital Equipment Corporation, Hudson, MA*, vol. 21, 1984.